Bursa Uludağ University Journal of The Faculty of Engineering, Vol. 27, No. 2, 2022 RESEARCH

DOI: 10.17482/uumfd.1134555

DESIGN AND THERMODYNAMIC PERFORMANCE ANALYSIS OF AN AMMONIA-WATER ABSORPTION REFRIGERATION AND MICROTURBINE COMBINED SYSTEM

Ayse Fidan ALTUN *

Received: 22.06.2022 ; revised: 21.07.2022 ; accepted: 02.08.2022

Abstract: Integrating absorption chillers in cogeneration and trigeneration systems are beneficial for increasing energy efficiency and sustainability. Those systems have higher efficiency, lower emissions, and lower costs compared to conventional systems. Therefore, it is crucial to develop thermodynamic models to predict the energy behaviour of the system for efficient design. System design and extensive thermodynamic analysis were conducted for a microturbine-NH_3/H_2O absorption cold and power system. The microturbine with a 60 kW power capacity is the prime mover.14 kW absorption chiller is fed by exhaust gases coming from the waste heat recovery part of the microturbine. The thermodynamic properties of the fluid at various state points were determined. The first and second law efficiency of the system was presented for different design parameters such as evaporation, condensation, generation temperature of the absorption system, effectiveness of the condenser-evaporator heat exchanger, and the solution heat exchanger. The proposed system's energy utilization factor is 28.3%, representing a 43.5% efficiency increase relative to the sole microturbine cycle. In addition, if waste heat from the flue gases discharged from the turbine is not recovered, a tremendous amount of energy may be lost. Therefore, the application of combined energy systems is a vital solution for energy efficiency.

Keywords: Combined cooling and power, absorption, micro-turbine, energy efficiency

Amonyak-Su ile Çalışan Absorpsiyonlu Soğutma ile Mikrotürbin Kombine Sisteminin Tasarımı ve Termodinamik Performans Analizi

Öz: Absorpsiyonlu soğutma sistemlerinin kojenerasyon ve trijenerasyon sistemlerine entegre edilmesi, enerji verimliliğini ve çevresel sürdürülebilirliği artırmak için faydalıdır. Bu sistemler, geleneksel sistemlere kıyasla daha yüksek verime, daha düşük emisyona ve daha düşük maliyete sahiptirler. Bu nedenle, sistemin enerji performansını öngörebilmek ve verimli sistemler tasarlayabilmek için termodinamik modeller geliştirmek çok önemlidir. Bu çalışmada, kombine bir mikro türbin ve NH_3/H_2O absorpsiyonlu soğutma sistemi için tasarım ve kapsamlı termodinamik analiz yapılmıştır. 60 kW güç kapasiteli mikro türbin, sistemin temel güç kaynağıdır. 14 kW kapasitesindeki absorpsiyonlu soğutucu, mikro türbinin atık ısı geri kazanım kısmından gelen egzoz gazları ile beslenmektedir. Sistemin çeşitli kontrol noktalarında, akışkanların termodinamik özellikleri belirlenmiş ve sunulmuştur. Sistemin birinci ve ikinci kanun verimi farklı tasarım parametreleri için hesaplanmıştır. Önerilen kombine sistemin enerji kullanım faktörü %28,3 olup , tekil bir mikrotürbin sistemi ile kıyaslandığında %43,5 daha yüksek verime sahiptir. Ayrıca türbinden atılan egsoz gazlarının ısısı geri kazanılmazsa çok büyük miktarda enerji kaybı olacaktır. Bu nedenle, birleşik enerji sistemlerinin uygulanması enerji verimliliği için hayati bir çözümdür.

Anahtar Kelimeler: Kombine soğutma ve güç, absorpsiyon, mikrotürbin, enerji verimliliği

* Orhangazi Yenikoy Asil Celik Vocational School, Bursa Uludag University, Bursa 16850, Turkey
Corresponding Author: Ayşe Fidan Altun (aysealtun@uludag.edu.tr)

NOMENCLATURE

Abbreviations		c	compressor
CCP	Combined cooling and power	cb	combustion
CCHP	Combined cooling, heating and power	con	condenser
CEHX	Condenser-Evaporator heat exchanger	evap	evaporator
CHP	Combined heat and power	f	fuel
COP	Coefficient of performance	g	generator
EUF	Energy utilization factor	p	pump
LHV	Lower heating value	pt	energy efficiency of the cycle using waste heat
MT	Microturbine	r	rectifier
SHX	Solution heat exchanger	T	turbine
Subscripts		v1	absorber throttle valve
a	absorber	v2	evaporator throttle valve

1. INTRODUCTION

Due to the rapid increase in global energy consumption, people seek alternative energy utilization ways. Recovering waste heat is one of the potential ways to provide available energy (Wang et al., 2016). In recent years, the combined systems that combine heat and power (CHP), cold and power (CCP), or cooling, heating and power (CCHP), have gained increasing attention since energy efficiency is a global concern. Those systems have several advantages, such as higher overall efficiency, lower greenhouse gas emissions, lower costs, and energy reliability compared to conventional systems (Chu et al., 2019). A traditional cogeneration unit comprises a prime mover and a heat recovery system. Combined systems mainly generate heating and cooling loads using the recovered heat (Mirzaee et al., 2019). Prime movers have various options; however, microturbines (MT) are becoming very popular. The microturbines are small power capacity combustion turbines, with powers ranging between 20 to 200 kWe (Huicochea et al., 2011). Microturbines offer high power density (Çakmak and Kılıç, 2007). Also, microturbines are able to operate with a variety of fuels such as natural gas, diesel fuel, gasoline, biogas, etc. Application of MT with absorption or adsorption cooling systems is also very efficient. The waste heat of the MT can be used to drive the absorption chiller.

Many researchers have conducted thermodynamic analyses of combined systems. Huicochea et al. (2011) investigated the energy performance of a trigeneration system comprised of a MT and a LiBr/water absorption chiller. Various operation conditions such as ambient temperature, fuel mass flow rate, and generation temperature were analyzed by the authors. Sun and Xie (2010) investigated experimentally the performance of a cold and power system that utilizes a 24.6 kW rated capacity MT as the prime mover. Results of the study revealed that the system does not save primary energy when the electric output is less than 10 kW. Herrera et al. (2014), investigated the thermo-economic performance of a cogeneration application with a reciprocating diesel engine as the prime mover and ammonia-water absorption system for cold production. The exhaust gases of the reciprocating engine are the energy source of the absorption chiller. The hydrogen concentration of the hydrogen-diesel oil blend and the different load conditions are the parameters investigated in the study. Mirzaee et al. (2019) studied the performance of a cogeneration system, including a gas turbine, absorption chiller, boiler, and heat exchangers. Various scenarios were created and investigated. The optimum scenario was determined based on the amount of carbon dioxide production, energy efficiency, and the utility fuel ratio. Thu et al. (2016) studied the performance of a micro-cogeneration system that uses a 65 kW electrical capacity MT as the prime mover coupled with a waste heat

recovery system. Second law analysis is used to find the exergy destructions of each component, and based on the results combustor is found to be responsible for most of the exergy destruction. Doseva and Chakyrova (2015) investigated the thermodynamic efficiency of an internal combustion engine-based cogeneration system that uses biogas from a wastewater treatment plant. Energy and exergy performance of the components, system efficiency, and power-to-heat ratio are some of the performance indicators used in the study. Results of the study showed that minor improvements in engine operation parameters could help increase the thermodynamic performance of the system. Kordlar and Akbari (2017) proposed a novel cooling and power cogeneration system driven by geothermal water. The proposed system is the combination of an Organic Rankine cycle and an ammonia-water absorption refrigeration system. The system configuration is optimized based on maximum first and second law efficiencies and minimum total product cost. Javanshir et al. (2020) investigated a cogeneration cycle for power and cooling. The proposed system is a combination of a Kalina cycle and absorption refrigeration cycle using an ammonia-water solution as the working fluid. To find out optimum working conditions, various operating conditions such as turbine inlet pressure, evaporator and condenser pressures are studied to see their influence on the cycle performance. Kazemiani et al. (2022) presented a novel ammonia-water cogeneration system driven by waste heat recovery. The authors investigated the impacts of the parameters such as ammonia concentration and the maximum pressure of the cycle on the system performance. Shankar and Rivera (2020) proposed an integrated power and cooling cycle operated by ammonia water as the working fluid. Kalina cycle and a vapour absorption refrigeration system are used in the study. Solar collectors provide hot water to the system. Analysis was done for different operating conditions such as hot fluid supply temperature, strong solution concentration, ammonia vapour concentration, etc.

From the above literature review, it can be understood that combined power and cooling systems are an essential concern in using available energy sources effectively. Also, based on the literature explained above, it seems that there is a lack of knowledge regarding ammonia-water power and cooling systems. This paper aims to study the integration of a microturbine and a single-effect ammonia-water absorption system. A multi-generation system that includes a microturbine as the driving unit, absorption chiller, and heat exchangers were introduced and modelled in EES software. A heat recovery system is designed to recover the energy of the exhaust gases exiting the microturbine. The recovered heat is utilized in the generator part of the absorption chiller. In addition, exhaust gases leaving the generator can be further used to provide hot water to the system. Various scenarios were created and analyzed to investigate and enhance the overall thermal efficiency of the combined systems.

The present work is an effort to address the lack of information regarding the design and performance evaluation of microturbine and ammonia-water absorption combined systems. Some significant contributions presented in this article are listed below:

- A comprehensive thermodynamic model was developed for the combined system. In order to increase the cycle efficiency, various additional components such as recuperator and condenser-evaporator heat exchanger are included.
- The properties at various state points were presented using the developed thermo-dynamic model
- The impact of effective parameters such as evaporation, condensation, and generation temperature of the absorption system, effectiveness of the condenser-evaporator heat exchanger, and solution heat exchanger on the system performance was investigated.

2. SYSTEM DESCRIPTION

The system comprises a prime mover, which is a microturbine, a heat recovery system and an absorption chiller. The chiller provides the cooling load using the recovered heat. A microturbine power system, which consists of a compressor, a combustion chamber, and a turbine, is implemented. For the microturbine section of the system, dry air enters the compressor, and after the compression process, the air enters the combustion chamber. In the chamber, compressed air and natural gas are combusted. Hot exhaust gases exiting the chamber enter the turbine to convert kinetic energy into mechanical energy. Exhaust gas exiting the recuperator enters the waste heat recovery system and provides thermal energy to the absorption chiller. The detailed configuration of the proposed integrated power and cooling system is presented in Fig.1.

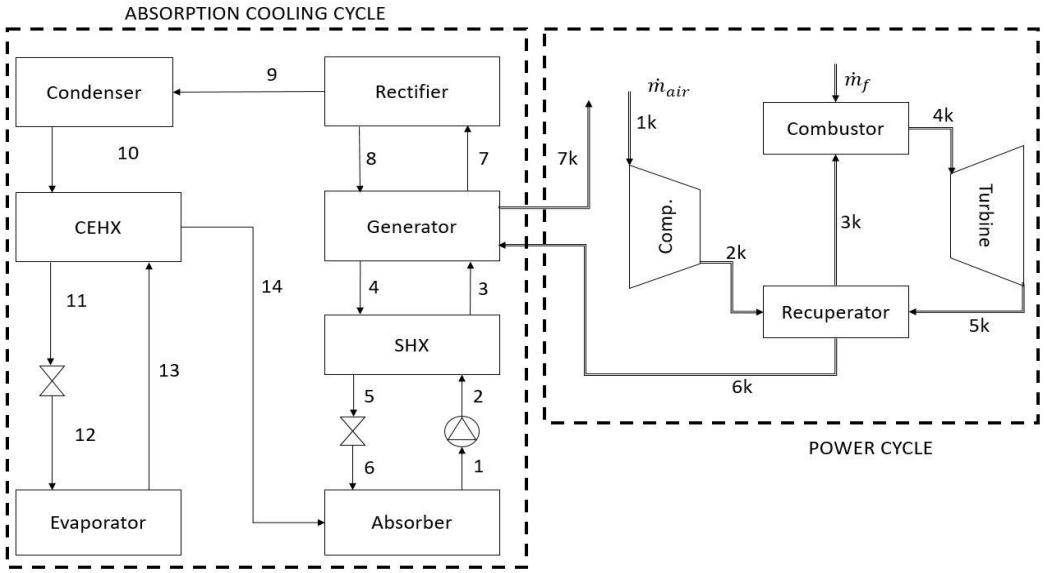

Figure 1:
Scheme of the combined microturbine-NH_3/H_2O absorption cooling system

Absorption chillers are thermally driven chillers that are suitable for the use of exhaust heat from microturbines. There are different types of absorption chillers, such as single, double and triple effect chillers. The absorption cooling system involves the absorption of a refrigerant by a transport medium. LiBr/water and Ammonia/water systems are two common absorbent and refrigerant pairs. Though, LiBr/water system has a limited range of operation due to crystallization (Seyfouri and Ameri, 2012). Ammonia-water systems are the most widely used systems, where ammonia serves as the refrigerant and water as the transport medium (Keçeciler et al., 2000). Ammonia refrigerant and water-absorbent working fluids are highly stable for a wide range of operating temperatures and pressure. Considering their broad evaporation temperature range (-60 °C ~10°C), ammonia-water systems can be used for many different applications such as comfort cooling for buildings, process refrigeration for industrial applications, etc. (Sun et al., 2013). In this study, a single effect, ammonia-water absorption chiller, is considered.

The single-stage ammonia-water absorption system has four main components, namely the generator, absorber, evaporator and condenser. There are also other auxiliary components such as expansion valves, a solution heat exchanger (SHX), condenser-evaporator heat

exchanger (CEHX), rectifier, and pump. The generator separates water and ammonia by vaporizing the ammonia. The rectifier completely purifies the ammonia vapour and directs the pure ammonia towards the condenser. Condensed ammonia leaves the condenser and passes through the condenser-evaporator heat exchanger. In the condenser-evaporator heat exchanger, the refrigerant that leaves the condenser subcools, using the cooler stream exiting the evaporator, heating the stream at the absorber inlet (Herold et al., 2016). High-pressure water from the generator returned to the absorber. Liquid ammonia vaporizes during the cooling process in the evaporator and enters the absorber. Water absorbs the ammonia and forms a strong ammonia solution in the absorber.

3. MATHEMATICAL MODELLING

To investigate the performance of the combined system, a comprehensive model is built based on the mass, energy and exergy balance. The model has been developed with EES software. This software has function libraries that include NH_3-water solutions. The developed system model is based on the assumptions below:

- The system analysis is conducted under steady-state condition
- Heat losses and pressure drops are neglected
- Two pressure levels were considered for the absorption cooling cycle: one for the condenser and generator, the other for the evaporator and the absorber (Martínez et al., 2016).
- Ammonia leaves the condenser as a saturated liquid.
- Ammonia leaves the evaporator as saturated steam.
- The isentropic efficiency of the pump is assumed as 0.5
- The effectiveness of the condenser-evaporator heat exchanger and the solution heat exchanger are assumed as 0.95 for the base case.
- Isentropic efficiency of the compressor and the turbine are 0.85 and 0.90, respectively.
- The effectiveness of the recuperator is assumed as 0.90.

The mass balance equation is shown below:

$$\sum \dot{m}_{in} = \sum \dot{m}_{out} \tag{1}$$

In Eq. (1), $\dot{m}$ is mass flow rate, *in* and *out* stands for inlet and exit states. The overall energy balance can be shown as in Eq.(2):

$$\dot{Q} + \sum \dot{m}_{in} h_{in} = \dot{W} + \sum \dot{m}_{out} h_{out} \tag{2}$$

$\dot{Q}$ and $\dot{W}$ are the net heat input and net work output, respectively. h_{in} and h_{out} are the entering and exiting enthalpy. The net heat input and work output can be calculated as below:

$$\dot{Q} = \dot{Q}_{net,in} = \dot{Q}_{in} - \dot{Q}_{out} \tag{3}$$

$$\dot{W} = \dot{W}_{net,out} = \dot{W}_{out} - \dot{W}_{in} \tag{4}$$

The exergy balance of the system can be expressed as below:

$$\sum \dot{X}_{in} - \sum \dot{X}_{out} + \sum \dot{Q} \left(1 - \frac{T_0}{T}\right) - \dot{W} - \dot{XD} = 0 \tag{5}$$

Where $\dot{X}_{in}$ and $\dot{X}_{out}$ represent net exergy input and output rate, respectively. $\dot{Q}$ is the heat transfer rate at temperature *T*, and $(\dot{X}D)$ is exergy destruction.

The exergy rate is given by:

$$\dot{X} = \dot{m}\Psi \tag{6}$$

In Eq.(6), Ψ represents the specific exergy flow, and it is given by:

$$\Psi = (\mathrm{h} - \mathrm{h}_0) - T_0(s - s_0) \tag{7}$$

In Eq.(7), temperature, enthalpy, and entropy in the dead state are shown as T_0, h_0, s_0, respectively. The energy and exergy balance equations are applied with considering each component as control volume. In the equations below, sub-indices with numbers represent corresponding cycle state points shown in Fig.1.

3.1 Energy and exergy analysis for the absorption chiller

Mass and energy balance equations are given below for the absorber:

$$\dot{m}_1 = \dot{m}_{14} + \dot{m}_6 \tag{8}$$

$$\dot{m}_1 x_1 = \dot{m}_{14} x_{14} + \dot{m}_6 x_6 \tag{9}$$

$$\dot{m}_6 h_6 - \dot{Q}_a + \dot{m}_{14} h_{14} = \dot{m}_1 h_1 \tag{10}$$

Entropy generation of the absorber:

$$\dot{S}_a = \dot{m}_1 s_1 - \dot{m}_6 s_6 - \dot{m}_{14} s_{14} + \frac{\dot{Q}_a}{T_0} \tag{11}$$

Mass and energy balance equations are given below for the pump:

$$\dot{W}_p = \frac{\dot{m}_1 v_1 (P_2 - P_1)}{\eta_P} \tag{12}$$

$$\dot{m}_1 h_1 = \dot{m}_2 h_2 - \dot{W}_p \tag{13}$$

Entropy generation of the pump:

$$\dot{S}_p = \dot{m}_2 s_2 - \dot{m}_1 s_1 \tag{14}$$

Mass and energy balance equations are given below for the solution heat exchanger

Effectiveness of the solution heat exchanger:

$$\varepsilon_{SHX} = \frac{T_4 - T_5}{T_4 - T_2} \quad (15)$$

$$\dot{m}_4 h_4 + \dot{m}_2 h_2 = \dot{m}_5 h_5 + \dot{m}_3 h_3 \quad (16)$$

Entropy generation of the solution heat exchanger:

$$\dot{S}_{SHX} = \dot{m}_5 s_5 + \dot{m}_3 s_3 - \dot{m}_4 s_4 - \dot{m}_2 s_2 \quad (17)$$

Mass and energy balance equations are given below for the generator

$$\dot{m}_8 + \dot{m}_3 = \dot{m}_7 + \dot{m}_4 \quad (18)$$

$$\dot{m}_3 x_3 + \dot{m}_8 x_8 = \dot{m}_7 x_7 + \dot{m}_4 x_4 \quad (19)$$

$$\dot{S}_g = \dot{m}_7 s_7 + \dot{m}_4 s_4 - \dot{m}_3 s_3 - \dot{m}_8 s_8 - \frac{\dot{Q}_g}{T_g} \quad (20)$$

Mass and energy balance equations are given below for the absorber throttle valve**:**

$$\dot{m}_6 = \dot{m}_5, x_6 = x_5 \quad (21)$$

$$h_6 = h_5 \quad (22)$$

$$\dot{S}_{VI} = \dot{m}_6 s_6 - \dot{m}_5 s_5 \quad (23)$$

Mass and energy balance equations are given below for the condenser**:**

$$\dot{m}_9 = \dot{m}_{10}\ , x_9 = x_{10} \quad (24)$$

$$\dot{m}_9 h_9 = \dot{m}_{10} h_{10} + \dot{Q}_{con} \quad (25)$$

$$\dot{S}_{con} = \dot{m}_{10} s_{10} - \dot{m}_9 s_9 + \frac{\dot{Q}_{con}}{T_0} \quad (26)$$

The effectiveness of the condenser-evaporator heat exchanger can be found as follows:

$$\varepsilon_{cehx} = \frac{T_{10} - T_{11}}{T_{10} - T_{13}} \quad (27)$$

$$\dot{m}_{10} h_{10} + \dot{m}_{13} h_{13} = \dot{m}_{11} h_{11} + \dot{m}_{14} h_{14} \quad (28)$$

Entropy generation can be calculated as:

$$\dot{S}_{cehx} = \dot{m}_{11} s_{11} + \dot{m}_{14} s_{14} - \dot{m}_{10} s_{10} - \dot{m}_{13} s_{13} \quad (29)$$

Mass and energy balance equations are given below for the evaporator throttle valve:

$$\dot{m}_{11} = \dot{m}_{12}, x_{11} = x_{12} \quad (30)$$

$$h_{11} = h_{12} \quad (31)$$

$$\dot{S}_{V2} = \dot{m}_{12}s_{12} - \dot{m}_{11}s_{11} \tag{32}$$

Mass and energy balance equations are given below for the evaporator:

$$\dot{m}_{12} = \dot{m}_{13},\ x_{12} = x_{13} \tag{33}$$

$$\dot{m}_{13}h_{13} = \dot{m}_{12}h_{12} + \dot{Q}_{evap} \tag{34}$$

$$\dot{S}_{evap} = \dot{m}_{13}s_{13} - \dot{m}_{12}s_{12} - \frac{\dot{Q}_{evap}}{T_0} \tag{35}$$

Mass and energy balance equations are given below for the rectifier:

$$\dot{m}_7 = \dot{m}_9 + \dot{m}_8 \tag{36}$$

$$\dot{m}_7x_7 = \dot{m}_9x_9 + \dot{m}_8x_8 \tag{37}$$

$$\dot{m}_7h_7 = \dot{m}_9h_9 + \dot{m}_8h_8 + \dot{Q}_r \tag{38}$$

$$\dot{S}_r = \dot{m}_8s_8 + \dot{m}_9s_9 - \dot{m}_7s_7 + \frac{\dot{Q}_r}{T_0} \tag{39}$$

3.2 Microturbine modelling

The microturbine subsystem works based on the Brayton cycle. The pressurization of the air can be done by a compressor. In order to pressurize the air, the compressor requires mechanical energy. Around 55-60% of the generated power by the turbine is internally used by the compressor (Mirzaee et al., 2019). Consumed power by the compressor can be calculated as below:

$$\dot{W}_C = \dot{m}_{air}(h_{C,out} - h_{C,in}) \tag{40}$$

Where, $\dot{m}_{air}$ is the mass flow rate of the air, $h_{C,out}$ is the enthalpy at the outlet, and $h_{C,in}$ is the enthalpy at the inlet of the compressor. The outlet pressure of the compressor can be calculated by using the pressure ratio r_C :

$$P_2 = r_C P_1 \tag{41}$$

Input mass flow rate to the turbine can be defined as:

$$\dot{m}_{T,in} = \dot{m}_{air} + \dot{m}_f \tag{42}$$

where $\dot{m}_f$ is the mass flow rate of the fuel. The power output of the turbine is:

$$\dot{W}_T = \dot{m}_{T,in}\left(h_{T,in} - h_{T,out}\right) \tag{43}$$

Where, $h_{T,out}$ is the enthalpy at the outlet, and $h_{T,in}$ is the enthalpy at the inlet of the turbine. The net power output of the system can be calculated as :

$$\dot{W}_{net} = \dot{W}_T - \dot{W}_c \tag{44}$$

3.3 System performance indicators

In this paper, the solution heat exchanger, condenser-evaporator heat exchanger, recuperator effectiveness, and the temperature of the evaporator, condenser, and generator were varied to evaluate their effect on net power and cooling output, and system efficiency.

The coefficient of performance for a single effect absorption chiller can be defined by the equation below:

$$COP = \frac{\dot{Q}_{evap}}{\dot{Q}_g + \dot{W}_p} \tag{45}$$

The efficiency of the microturbine subsystem is given in Eq.(46):

$$\eta_P = \frac{\dot{W}_{net}}{\dot{m}_f \times LHV \times \eta_{cb}} \tag{46}$$

With $\dot{m}_f$ and *LHV* represents the fuel mass flow rate and the lower heating value of the Natural Gas. η_{cb} is the combustion efficiency which assumed as 0.95. LHV of the natural gas is taken as 50,023 kJ/kg. In cogeneration systems, there are two types of energy output. The energy products are power and cooling for the proposed cycle. The energy utilization factor *(EUF)* can be expressed in Eq.(47):

$$EUF = \frac{\left(\dot{W}_{net} + \dot{Q}_{evap}\right)}{\dot{m}_f \times LHV \times \eta_{cb}} \tag{47}$$

Where $\dot{W}_{net}$ is the system's net output power, $\dot{Q}_{evap}$ is the produced cooling by the evaporator. The energy efficiency of the cycle can also be defined by using waste heat energy utilized in the generator ($\dot{Q}_{heat}$):

$$\eta_{PT} = \frac{\left(\dot{W}_{net} + \dot{Q}_{heat}\right)}{\dot{m}_f \times LHV \times \eta_{cb}} \tag{48}$$

The second law efficiency of the whole system can be defined as the ratio of the useful exergy produced by the system to the fuel exergy supplied to the system. In this equation, the fuel exergy is assumed to be equal to the LHV of the natural gas.

$$\eta_{ex,CCP} = \frac{\left(\dot{W}_{net} + \left(\dot{Q}_{heat}\left(1 - \frac{T_0}{T}\right)\right)\right)}{\dot{m}_f \times LHV \times \eta_{cb}} \tag{49}$$

4. RESULTS AND DISCUSSION

4.1 Model Validation

Data available from the literature are used to validate the absorption model which was used to run under the same operating conditions as in the work of (Adewusi and Zubair, 2004). For the considered single-stage ammonia-water absorption system, the mass flow rate through the solution pump is 1 kg/s, the saturated liquid leaving the condenser and the absorber is at 40°C, and the evaporator outlet saturation temperature is -10 °C. In Table 1, a comparison of thermodynamic analysis results of the present study and the results of the study of Adewusi and Zubair are given. It can be seen that the agreement between the results is very well.

Table 1. Comparison of the present model calculation results with the study of Adewusi and Zubair (2004)

Component	Heat Transfer Rate or Power [kW]			Entropy Generation [kW/K]		
	Adewusi and Zubair	Present Study	Difference Rate (%)	Adewusi and Zubair	Present Study	Difference
Generator	267.9	263.9	-1.51	0.0128	0.0127	-0.78
Rectifier	50.7	49.2	-3.04	0.0304	0.0302	-0.66
Absorber	231.0	227.2	-1.67	0.0774	0.0777	0.38
Pump	3.0	3.04	1.31	0.0048	0.0048	0
Condenser	151.0	156.0	3.2	0.0341	0.0358	4.7

4.2 Performance of the base case

The temperature, pressure, and mass flow rate data for the absorption and microturbine subsystem are given in Table 2 and Table 3.

- The work of the compressor ($\dot{W}_C$), turbine ($\dot{W}_T$) and the system net power ($\dot{W}_{net}$) are determined to be 27.4 kW, 60 kW, 32.6 kW, respectively.
- The heat rate of the evaporator and the generator were calculated as 14.07 kW, 20.96 kW, respectively.
- COP was found as 0.666, respectively.
- The energy efficiency of the microturbine subsystem is 0.198, whereas the energy utilization factor of the whole system is 0.284. The energy efficiency of the system, including the waste heat recovery, is 0.326. It is essential to highlight that, by utilizing the exhaust gas exiting the microturbine system in the generator part of the absorption chiller, the energy efficiency has increased by 43.1%.

In this paper, evaporator, condenser and generator temperature and the heat exchanger effectiveness values are varied in order to evaluate their effect on the system performance. The parameters used for the parametric analysis are presented in Table 4.

In Fig.2, the comparison of the entropy generation between the absorption chiller components is given. A maximum entropy generation rate of 37% is seen in the absorber. After the absorber, the highest entropy generation occurs in the evaporator and the condenser. The exergy efficiency of the other components, such as the pump, and the heat exchangers, are relatively low. The total exergy efficiency of the absorption chiller is 14.41%.

Table 2. The thermophysical properties at various state points and energy rates for the absorption subsystem.

State no	$\dot{m}$ [kg/s]	T [C]	x_i (kg/kg sol)	P_i [kPa]	h_i [kJ/kg]	s_i [kJ/kg.K]
1	0.0569	40.00	0.4588	409.2	-59.42	0.443
2	0.0569	40.41	0.4588	1556.00	-56.65	0.447
3	0.0569	100.3	0.4588	1556.00	214.3	1.239
4	0.0449	120.00	0.3145	1556.00	333.30	1.509
5	0.0449	44.39	0.3145	1556.00	-10.04	0.539
6	0.0449	43.08	0.3145	409.2	-10.04	0.543
7	0.0125	89.47	0.9783	1556.00	1462	4.668
8	0.0005	89.47	0.4588	1556.00	166.5	1.109
9	0.0120	45.13	0.9996	1556.00	1311.00	4.223
10	0.0120	40.00	0.9996	1556.00	190.70	0.658
11	0.0120	18.88	0.9996	1556.00	88.31	0.319
12	0.0120	-1.27	0.9996	409.2	88.31	0.336
13	0.0120	0	0.9996	409.2	1261	4.629
14	0.0120	38.00	0.9996	409.2	1363	4.981

$\dot{Q}_{abs}$	19.29 kW	$\dot{Q}_{evap}$	14.07 kW
$\dot{Q}_{con}$	13.44 kW	$\dot{Q}_{rect}$	2.458 kW
$\dot{Q}_{des}$	20.96 kW	$\dot{Q}_{rhx}$	1.229 kW
$\dot{Q}_{shx}$	15.43 kW	COP	0.6662
$\eta_{ex,absorption}$	0.1441	$\dot{S}_{tot}$	0.01874 kW/K

Table 3. The thermophysical properties at various state points and energy rates for the microturbine subsystem

State no	Fluid	$\dot{m}$ [kg/s]	T [C]	P_i [kPa]	h_i [kJ/kg]	s_i [kJ/kg.K]
1k	Air	0.16	25	101.3	298.4	6.859
2k	Air	0.16	194.2	405.3	469.6	6.915
3k	Air	0.16	621.9	405.3	927.9	7.608
4k	Air	0.1635	1000	397.2	1348	8.007
5k	Air	0.1635	669.4	101.3	981.3	8.064
6k	Air	0.1635	255.2	101.3	532.6	7.44
7k	Air	0.1635	130	101.3	404.4	7.163

EUF	0.284	$\eta_{ex,CCP}$	0.203
η_P	0.198	$\dot{W}_{net}$	32.6 kW
η_{PT}	0.326	$\dot{W}_T$	60 kW
$\dot{W}_C$	27.4 kW		

Table 4. The parameters assumed for the parametric analysis

	Generator Temperature [°C]	Evaporator Temperature [°C]	Condenser Temperature [°C]	SHX effectiveness [-]	CEHX effectiveness [-]
Case 1	***115-150***	0	40	0.95	0.95
Case 2	120	0	***20-47***	0.95	0.95
Case 3	120	***(-8)-1***	40	0.95	0.95
Case 4	120	0	40	***0.1-0.9***	0.95
Case 5	120	0	40	0.95	***0.1-0.9***

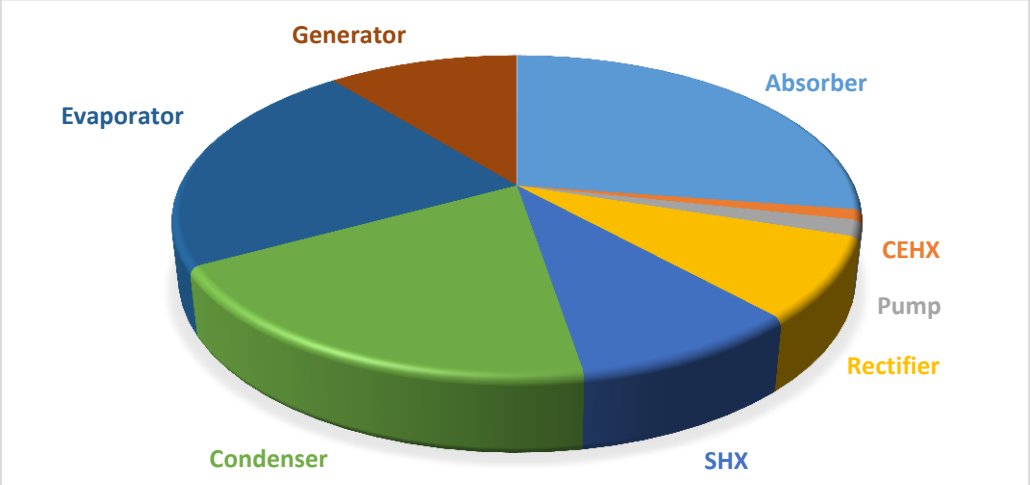

Figure 2:
The entropy generation of the absorption chiller components

4.3 The influence of the generator temperature

The energy utilization factor and the mass flow rate of the fuel against the generator temperature are plotted in Fig. 3. The evaporator temperature, condenser temperature, and the effectiveness of the heat exchangers are fixed. As can be seen in the figure, the EUF decreases with an increment of T_G . The mass flow rate of the fuel increases with an increment of T_G in order to provide a 14.07 kW cooling capacity. It seems that the influence of the T_G is more dramatic between 115 to 120 °C. Between 115 to 120 °C, the EUF decreases from 0.52 to 0.28. In Fig.4, the simulation results were given for entropy generation against the generator temperature. The figure illustrates that the entropy generation of the absorption chiller increases by 27% between 115 to 150 °C generator temperature.

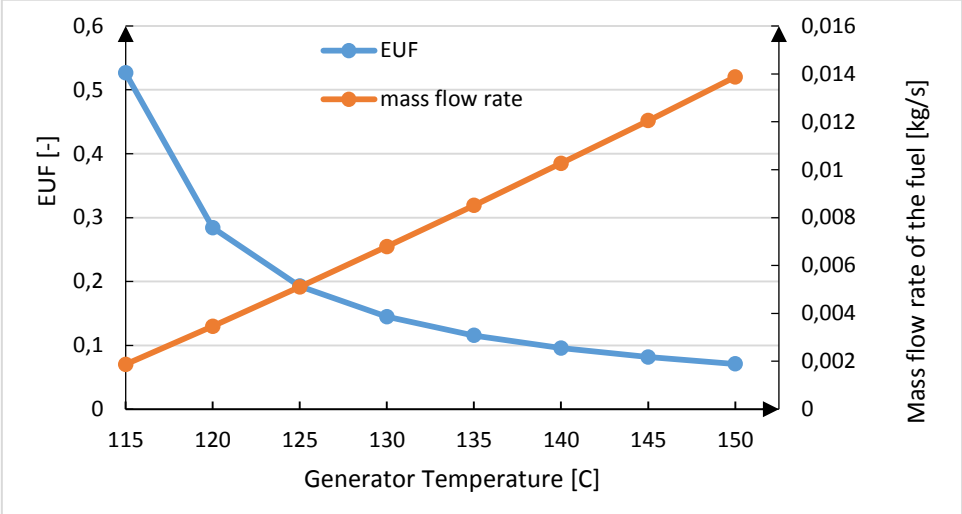

Figure 3:
The influence of generator temperature on the EUF and mass flow rate of the fuel

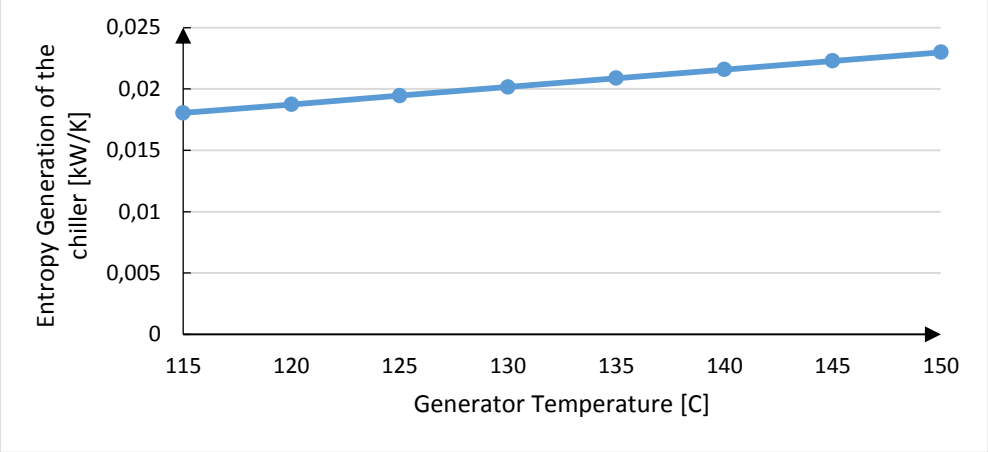

Figure 4:
The influence of generator temperature on the entropy generation of the absorption chiller

4.4 The influence of the evaporator temperature

Fig. 5 shows the effect of the evaporator temperature on the COP (T_G is fixed at 120°C). Results show that an increase in the evaporator temperature results in an increase in COP values. Between -8 to 1 °C of evaporator temperature, the COP of the absorption chiller increases by 10.3%. Fig.6 depicts the effect of the T_{evap} on the exergy efficiency of the absorption chiller ($\eta_{ex,absorption}$) and the total entropy generation by the chiller. Exergy efficiency increases, and the total entropy generation by the chiller decreases with an increase in the evaporator temperature. As can be seen in Fig. 7, all of the defined efficiencies are increased for greater values of evaporator temperature. For -8°C of T_{evap}, EUF, and η_{PT} have the values of 0.144 and 0.378; for 1°C of T_{evap}, EUF have the value of 0.3184, and η_{PT} has the value of 0.81.

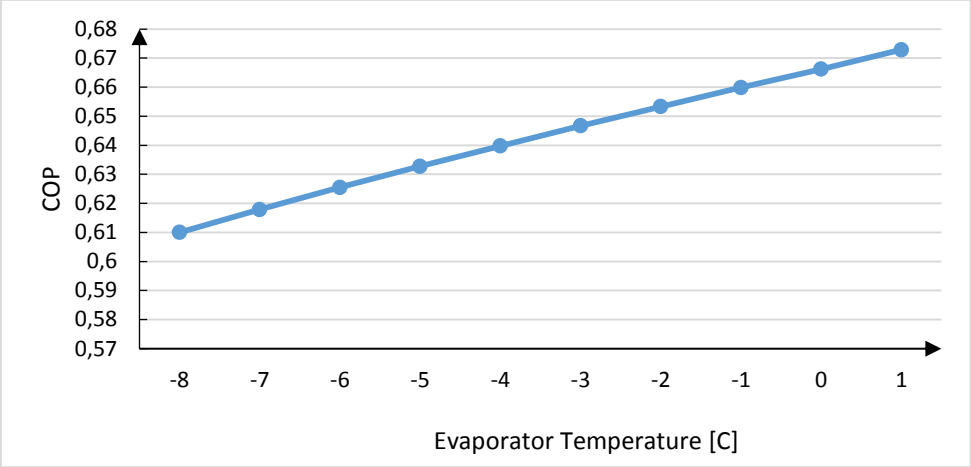

Figure 5:
The influence of the evaporator temperature on the COP

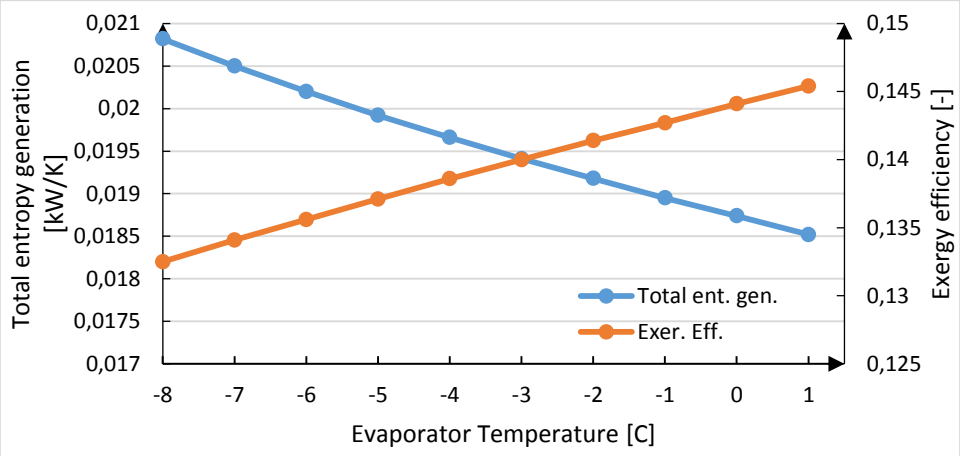

Figure 6:
The influence of the evaporator temperature on entropy generation and the exergy efficiency

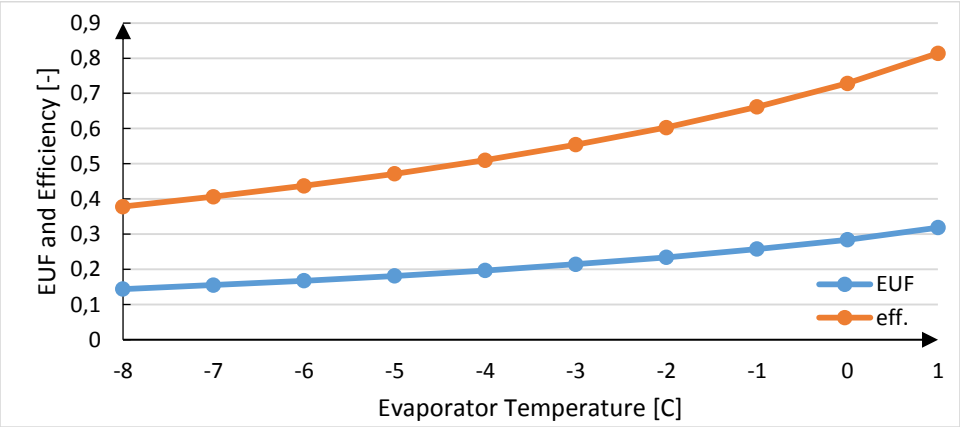

Figure 7:
The influence of the evaporator temperature on EUF and system efficiency (η_{PT})

4.5 The influence of the condenser temperature

In this part of the study, the condenser temperature is varied from 20 to 47 °C to see its influence on the system behaviour. The generator temperature and the evaporator temperature are fixed at 120°C and 0°C, respectively. Fig.8 illustrates the effect of the condenser temperature on the COP and the cooling capacity of the absorption chiller. Results revealed that an increase in the condenser temperature results in a decrease in the COP. At higher condenser temperatures, the cooling capacity of the system decreases. At 20°C, the COP of the system is 0.705, and at 47°C, the COP of the system is 0.647. Similarly, Q_{evap} is 14.7 kW at 20°C, and it decreases to 13.83 kW at 47°C. Fig.9 depicts the exergy efficiency and entropy generation by the chiller versus varying condenser temperatures. The exergetic efficiency of the absorption chiller decreases by 7.25%, and the entropy generation increases by 5.71% when the condenser temperature changes from 20 to 47 °C. Fig.10 shows the effect of the condenser temperature on the *EUF* and the energy efficiency using waste heat η_{PT}. Results reveal that all of the defined system efficiencies decrease with increasing condenser temperature.

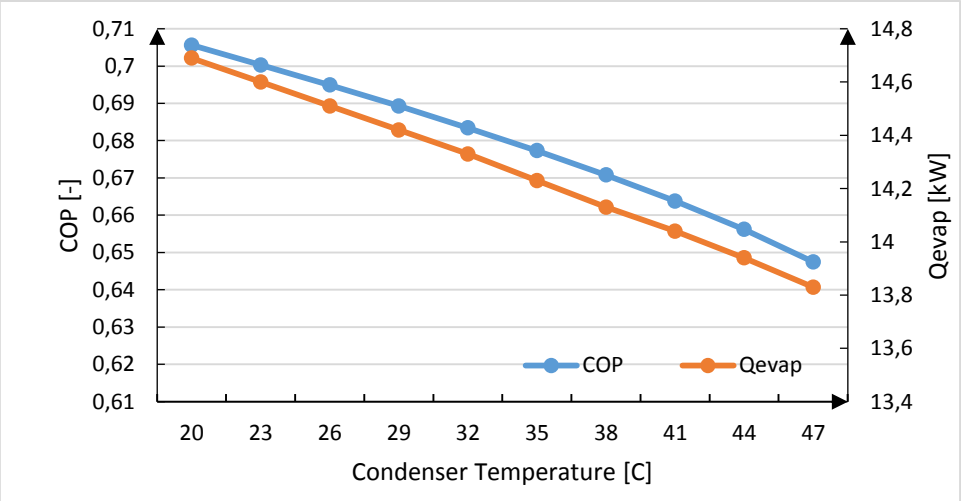

Figure 8.:
The influence of the condenser temperature on the COP and the cooling capacity (Q_{evap})

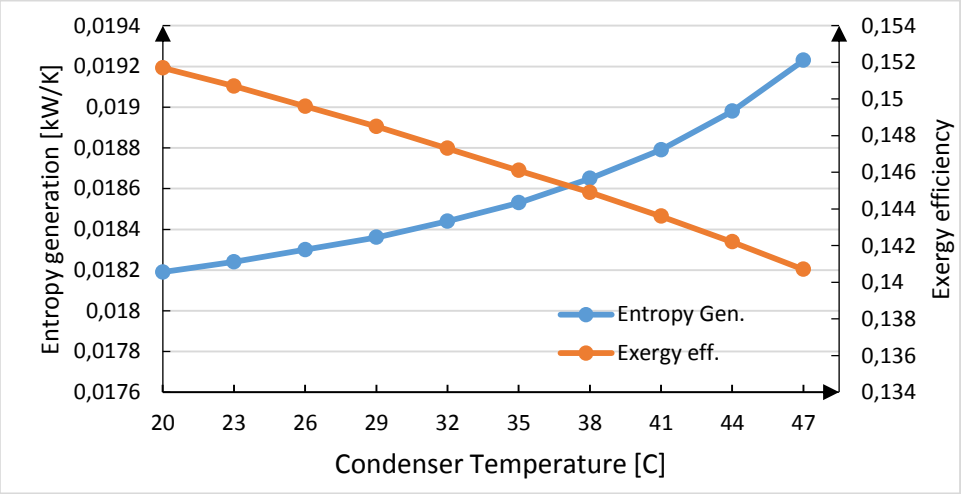

Figure 9:
The influence of the condenser temperature on the total entropy generation and the exergy efficiency

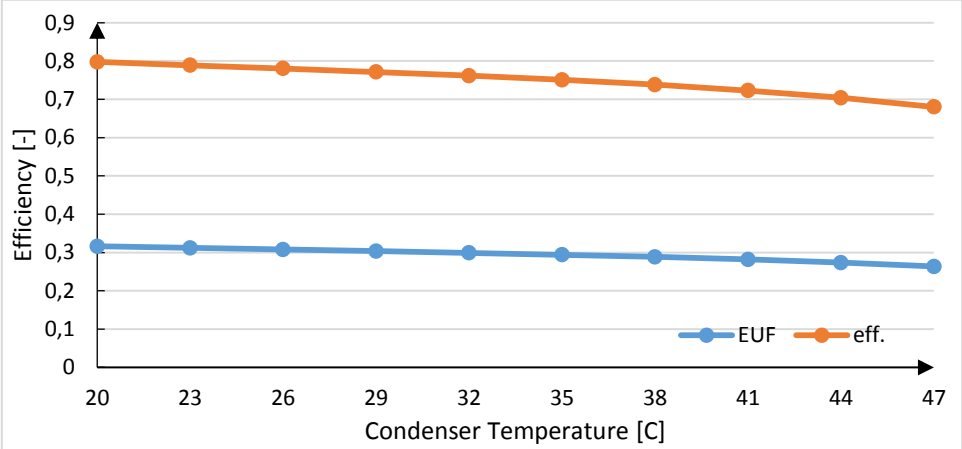

Figure 10:
The influence of the condenser temperature on the efficiencies

4.6 The influence of the solution heat exchanger effectiveness

The solution heat exchanger is an essential component in the system that leads to performance improvement. In the solution heat exchanger, the hot solution leaving the generator preheats the cold solution entering the generator. Due to this internal heat exchange, the external heat required to utilize the generator is reduced.

The solution heat exchanger effectiveness is varied from 0.1 to 0.9, and the COP of the chiller is given in Fig. 11. Other operating conditions have remained constant. Results revealed that the solution heat exchanger is a critical component, and its effectiveness influences the system performance in an outstanding manner. From 0.1 to 0.9 effectiveness, the COP of the system changes from 0.402 to 0.641. The effect of the solution heat exchanger effectiveness on the entropy generation of the chiller and the exergy efficiency is presented in Fig.12. Results revealed that entropy generation decreases, and the exergy efficiency of the chiller increases for solution heat exchangers with higher effectiveness values. The entropy generation reduces by 36.7%, and the exergy efficiency increases by 59.7% when the effectiveness of the solution heat exchanger changes from 0.1 to 0.9. In Fig.13, the system efficiencies versus the solution heat exchanger effectiveness are presented. Simulation results highlight that the solution heat exchanger is a critical component, and it highly influences the whole system's efficiency. When the effectiveness is 0.1, the *EUF* is 0.035, and the energy efficiency using waste heat recovery is 0.108; when the effectiveness becomes 0.9, the *EUF* and the η_{PT} becomes 0.201, and 0.522, respectively.

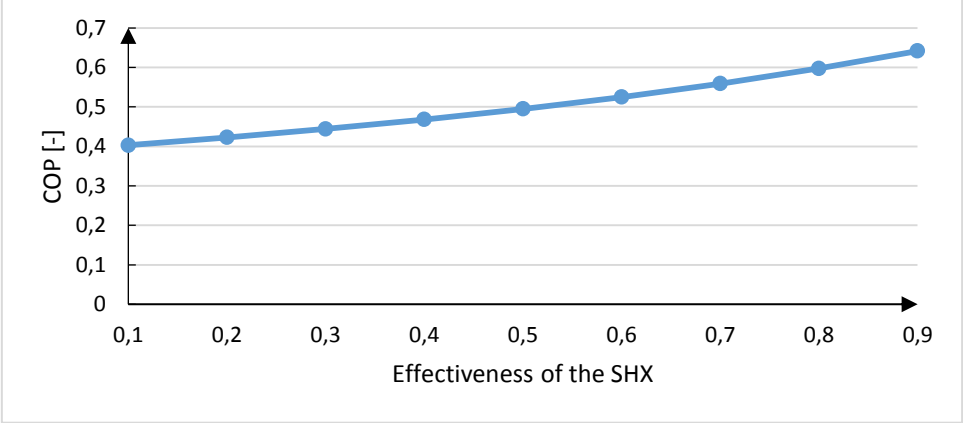

Figure 11:
The influence of the solution heat exchanger's effectiveness on the COP

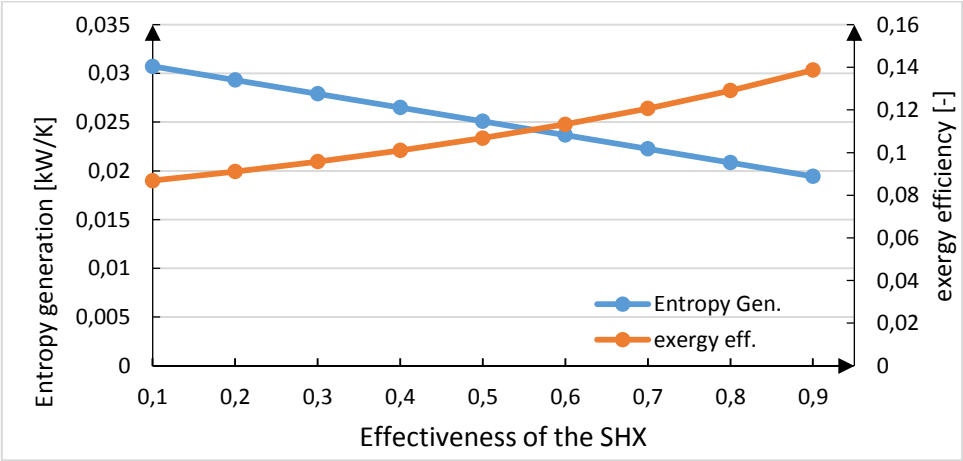

Figure 12:
The influence of the solution heat exchanger effectiveness on the entropy generation and the exergy efficiency

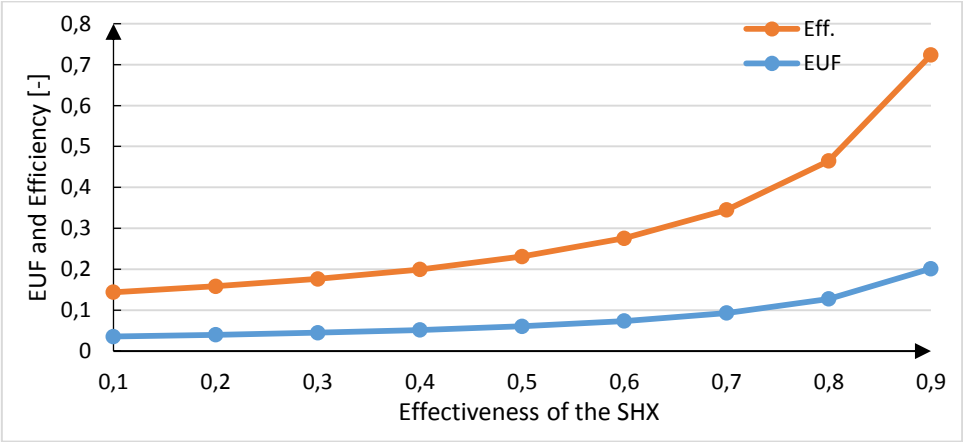

Figure 13:
The influence of the solution heat exchanger effectiveness on the system efficiencies

4.7 The influence of the CEHX effectiveness

Fig.14 illustrates the effect of the condenser evaporator heat exchanger (or condensate precooler) effectiveness on COP and the cooling capacity of the absorption chiller. The CEHX reduces the enthalpy at the inlet of the evaporator; therefore, the cooling capacity of the chiller increases. Results highlight that for higher CEHX effectiveness values, the system has more excellent COP and cooling capacity values. Therefore, applying a CEHX improves the system's performance. For a 0.1 heat exchanger effectiveness value, the cooling capacity of the chiller is 13 kW, and it becomes 14 kW for a 0.9 heat effectiveness value. In Fig. 15, the exergy efficiency of the chiller and the EUF is given. Between 0.1 to 0.9 effectiveness values, the exergy efficiency of the chiller increases by 7.41%, and the EUF increases by 2.12%. It can be concluded that despite the fact that the refrigerant heat exchanger has an influence on the efficiencies, it does not influence the system performance as much as the solution heat exchanger.

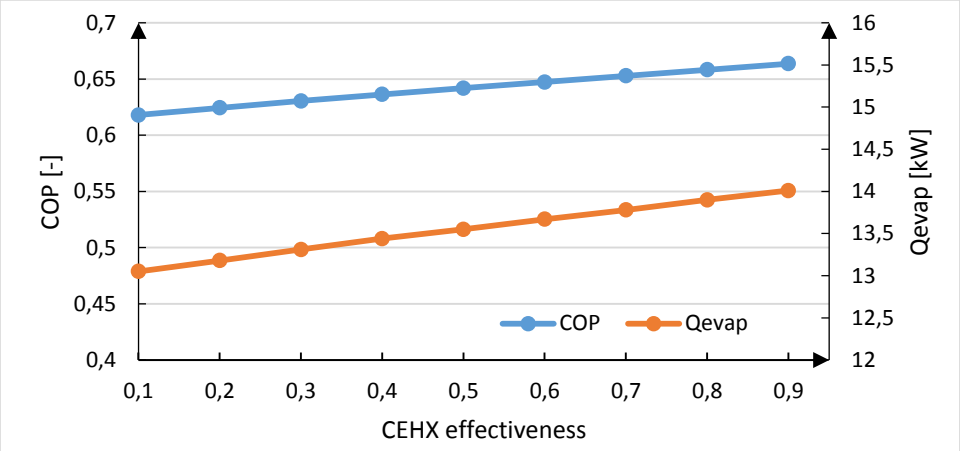

Figure 14:
The influence of the CEHX effectiveness on the COP and Q_{evap}

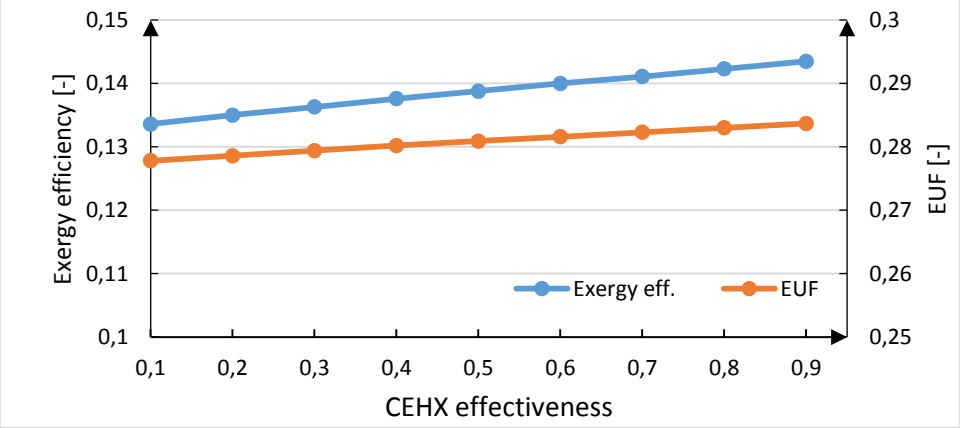

Figure 15:
The influence of the refrigerant heat exchanger's effectiveness on the exergy efficiency of the chiller and the EUF

5. CONCLUSIONS

Comprehensive thermodynamic modelling is carried out for a power/cooling combined system. The proposed system consists of an ammonia-water absorption chiller connected to a microturbine. The performance of the cycle is assessed to figure out the effects of various variables on the thermal and exergy efficiencies. The methodology includes (i) formulating the thermodynamic model using energy and exergy balance equations of the system components; (ii) determining the energy and exergy performance assessment indicators such as energy utilization factor, coefficient of performance, total entropy generation, and the exergy efficiency. The following conclusions were obtained:

- For the base case, the microturbine has a 60 kW power output, and after subtracting the compressor power input, the net power output from the system is 32.6 kW. With the utilization of the waste heat, a 14.07 kW cooling load can be provided by the evaporator.
- The base case's energy utilization factor is 28.3%, representing a 43.5% efficiency increase relative to a sole microturbine cycle. The exergy efficiency of the combined plant was estimated to be 20.3%.

- The increase of the generator temperature decreases the energy utilization factor because the mass flow rate of the fuel increases to provide the same power demand. The entropy generation by the chiller increases with increasing generator temperature.
- The increase of the evaporator temperature increases the COP, Energy utilization factor, and the exergy efficiency of the chiller and decreases the total entropy generation.
- The increase of the condenser temperature results in a decrease in the COP and the cooling capacity. The energetic efficiency decreases, and the entropy generation increases at higher condenser temperatures.
- The integration of the solution heat exchanger and condenser-evaporator heat exchanger was also investigated. Both of the heat exchangers enhance the thermal performance of the system. However, the solution heat exchanger has a dominant influence on the system efficiency. CEHX does not influence the system performance as much as the SHX.
- The results demonstrated that the system proposed in this paper is an attractive solution to produce cooling and power simultaneously. A sole microturbine system produces only power generation, and it has lower efficiency when compared to the proposed system. In addition, the waste heat from the flue gases discharged from the turbine is not recovered, and a significant amount of energy may be lost. Therefore, the application of combined energy systems is an energy-efficient and sustainable solution.

CONFLICT OF INTEREST

The author confirms that there is no known conflict of interest or common interest with any institution/organization or person.

AUTHOR CONTRIBUTION

Ayşe Fidan Altun takes all responsibility for the manuscript.

REFERENCES

1. Adewusi, S.A., Zubair, S.M. (2004). Second law-based thermodynamic analysis of ammonia-water absorption systems, *Energy Convers. Manag.*, 45, 2355–2369. https://doi.org/10.1016/j.enconman.2003.11.020

2. Akbari Kordlar, M., Mahmoudi, S.M.S. (2017). Exergeoconomic analysis and optimization of a novel cogeneration system producing power and refrigeration, *Energy Convers. Manag.*, 134, 208–220. https://doi.org/10.1016/j.enconman.2016.12.007

3. Çakmak, T., Kılıç, M. (2007). The Simulation of a Micro-gas Turbine Cycle and Optimization of the System Components, *Uludağ University Journal of The Faculty of Engineering*, 12, 97–108.

4. Chu, X., Yang, D., Li, J. (2019). Sustainability Assessment of Combined Cooling , Heating , and Power Systems under Carbon Emission Regulations, *Sustain.*, 11, 1–17. https://doi.org/10.3390/su11215917

5. Doseva, N., Chakyrova, D. (2015). Energy and exergy analysis of cogeneration system with biogas engines, *J. Therm. Eng.*, 1, 391–401. https://doi.org/10.18186/jte.75021

6. Herold, K.., Radermacher, R., Klein, S.A. (2016). Absorption Chillers and heat pumps, CRC Press.

7. Herrera, M.D.M., Arrieta, F.R.P., Sodré, J.R. (2014). Thermoeconomic assessment of an absorption refrigeration and hydrogen-fueled diesel power generator cogeneration system, *Int. J. Hydrogen Energy*, 39, 4590–4599. https://doi.org/10.1016/j.ijhydene.2014.01.028

8. Huicochea, A., Rivera, W., Gutiérrez-Urueta, G., Bruno, J.C., Coronas, A. (2011). Thermodynamic analysis of a trigeneration system consisting of a micro gas turbine and a double effect absorption chiller, *Appl. Therm., Eng.*, 31, 3347–3353. https://doi.org/10.1016/j.applthermaleng.2011.06.016

9. Javanshir, N., Seyed Mahmoudi, S.M., Kordlar, M.A., Rosen, M.A. (2020). Energy and cost analysis and optimization of a geothermal-based cogeneration cycle using an ammonia-water solution: Thermodynamic and thermoeconomic viewpoints., *Sustain.*, 12. https://doi.org/10.3390/su12020484

10. Kazemiani-najafabadi, P., Amiri, E., James, C. (2022). Designing and thermodynamic optimization of a novel combined absorption cooling and power cycle based on a water-ammonia mixture., *Energy*, 253, 124076. https://doi.org/10.1016/j.energy.2022.124076

11. Keçeciler, A., Acar, H.İ., Doğan, A. (2000). Thermodynamic analysis of the absorption refrigeration system with geothermal energy: An experimental study., *Energy Convers. Manag.*, 41, 37–48. https://doi.org/10.1016/S0196-8904(99)00091-6

12. Martínez, J.C., Martinez, P.J., Bujedo, L.A. (2016). Development and experimental validation of a simulation model to reproduce the performance of a 17.6 kW LiBr-water absorption chiller., *Renew. Energy*, 86, 473–482. https://doi.org/10.1016/j.renene.2015.08.049

13. Mirzaee, M., Zare, R., Sadeghzadeh, M., Maddah, H., Ahmadi, M.H., Acıkkalp, E., Chen, L. (2019). Thermodynamic analyses of different scenarios in a CCHP system with micro turbine – Absorption chiller, and heat exchanger., *Energy Convers. Manag.*, 198. https://doi.org/10.1016/j.enconman.2019.111919

14. Seyfouri, Z., Ameri, M. (2012). Analysis of integrated compression-absorption refrigeration systems powered by a microturbine., *Int. J. Refrig.*, 35, 1639–1646. https://doi.org/10.1016/j.ijrefrig.2012.04.010

15. Shankar, R., Rivera, W. (2020). Investigation of new cooling cogeneration cycle using NH_3–H_2O mixture., *Int. J. Refrig.*, 114, 88–97. https://doi.org/10.1016/j.ijrefrig.2020.02.014

16. Sun, L., Han, W., Jing, X., Zheng, D., Jin, H. (2013). A power and cooling cogeneration system using mid/low-temperature heat source., *Appl. Energy*, 112, 886–897. https://doi.org/10.1016/j.apenergy.2013.03.049

17. Sun, Z.G., Xie, N.L. (2010). Experimental studying of a small combined cold and power system driven by a micro gas turbine., *Appl. Therm. Eng.*, 30, 1242–1246. https://doi.org/10.1016/j.applthermaleng.2010.02.006

18. Thu, K., Saha, B.B., Chua, K.J., Bui, T.D. (2016). Thermodynamic analysis on the part-load performance of a microturbine system for micro/mini-CHP applications., *Appl. Energy*, 178, 600–608. https://doi.org/10.1016/j.apenergy.2016.06.106

19. Wang, J., Wang, J., Zhao, P., Dai, Y. (2016). Thermodynamic analysis of a new combined cooling and power system using ammonia-water mixture., *Energy Convers. Manag.*, 117, 335–342. https://doi.org/10.1016/j.enconman.2016.03.019